



ORIGINAL RESEARCH ARTICLE

NUMERICAL ANALYSIS OF A SEAMLESS MILD STEEL POLE FOR LOW AND MEDIUM-TENSION POWER TRANSMISSION LINE IN BORNO STATE NIGERIA

M. Shuwa^{1*}, U. A. Mukhtar¹, I. Mu'azu², M. I. Ishaq¹ and F. M. Kajiam¹

¹Department of Mechanical Engineering, University of Maiduguri, Maiduguri, Nigeria

²Federal Neuropsychiatric Hospital, Maiduguri, Nigeria

*Corresponding author's email: mshuwa@unimaid.edu.ng

ARTICLE INFORMATION

Received: 8th August 2025

Revised: 13th November 2025

Accepted: 14th November 2025

Keywords:

Numerical analysis
Pole
Stress
Aerodynamic load
Displacement

ABSTRACT

This work presents a computational method of evaluating structural performance of a seamless mild steel pipe material under various load conditions for supporting low and medium-tension power transmission lines. The low and medium tension power transmission line seamless mild steel (LMTPL-SMS) pole material was specifically analyzed for reliability and resilience considering the environmental and operational conditions of Borno State, Nigeria. Borno State's power infrastructure is subjected to significant challenges, one of which is stochastic wind loads due to harsh environmental factors. This threat has led to poles failure resulting in vandalism and power outages. To ensure the reliability and resilience of the power network, a robust pole structural design is critical. In this work a 9.7536m seamless mild steel pole material ASME SA-106 Grade B was selected based on availability and cost for analysis. COMSOL Multi-physics 5.2 numerical code was used to develop and analyze the behavior of the pole material based on predefined loading conditions and on the assumptions of Euler-Bernoulli's beam-column theory. Using the code's solid mechanics interface displacement and stress distribution response on the pole when subjected to static, dynamic and aerodynamic loads simultaneously were computed and analyzed at an excitation frequency of 110 GHz. The result shows a frequency response of the transfer function in terms of electric field norm of $3.7 \times 10^{-9} Vm^{-1}$ under the predefined loading conditions, which was greater than $8.5 \times 10^{-8} Vm^{-1}$ the response established by the manufacturers of the mild steel pipe material. The maximum stress recorded was $8.82 \times 10^7 N/m$ which is less than the $8 \times 10^8 N/m$ yield strength of the selected pole material. It was observed that the displacement is from 0m at the root to maximum value of 0.11m at the top. The maximum displacement recorded was 0.39m. This value is 22% less than the determined critical displacement of the pole material, which was 0.50m... Thus, the displacement was within the elastic limit of the pole material based on the defined geometry and boundary condition. Furthermore, the F-Test statistical tool used to validate these results with an experimental one carried out shows that there is no significant difference between the two results. Therefore, the analysis established that the selected pole material was reliable under the predefined simultaneously applied extreme loads, thus, the LMTPL-SMS pole will be suitable for use in Borno State, Nigeria, thus objective of the work was achieved.

© 2025 Faculty of Engineering, University of Maiduguri, Nigeria. All rights reserved.

1.0 Introduction

Reliable and sustainable electricity supply is fundamental to socio-economic development. In Nigeria, and particularly in the northeastern state of Borno, power infrastructure faces unique and severe challenges, including the destruction of transmission lines by difficult environmental conditions and insurgency. Following extended power outages, efforts have been made to restore and improve electricity supply, notably with the establishment of new generating projects. However, the resilience and structural integrity of the transmission

infrastructure, specifically the poles that support the power lines, remain a critical issue of concern. Electric transmission poles are unique structures that are used to support conductors and shield wires of a transmission line; could be either lattice type or pole type structures. Lattice type structures are used for high tension voltages while poles types are used for low to medium tension (Aliyu and Abejide, 2019). Materials used in power pole construction can be wood, reinforced concrete, steel or even composite materials, such as Fiber Reinforced Plastic or Fiber Reinforced Polymer (FRP) poles that are becoming more prevalent nowadays (Oyejide *et al*, 2014; Nweke *et al*, 2017; Aliyu and Abejide, 2019). In recent years, utility providers have been searching for most cost-effective alternatives to timber poles and other pole materials due to environmental concerns, high cost of maintenance, and need for improved aesthetics. However, steel poles are considered to be the strongest material used in power pole construction that require less maintenance than the other varieties. interestingly, choosing the correct steel grade and geometry for peculiar geography and application is still a subject of concern and consequently of great significance (WAPA, 2021; Puwo, 2024). An electric steel pole acts as a cantilever structure, which is designed and analyzed as a tapered member with combined axial and bending loads. The forces acting on the poles are from the vertical loading (comprising dead weight of conductors, cross arms, insulators) and the horizontal loading due to wind pressure on conductors and pole. Horizontal loading is the most cause of failure of transmission poles especially in areas associated with stochastic winds (Wagner and Mathur, 2018; WAPA, 2021).

Borno State located between approximately latitude 10°N and 14°N and longitude 11°30'E and 14°45'E in North-east Nigeria is associated with stochastic winds with an average wind speed of 3.89m/s (Ngala *et al*, 2015; Shuwa *et al*, 2016). The state is the second largest state in the country with 27 local government areas and more than half of these local governments are not connected to the national grid. Lack of stable and steady power supply has greatly affected sustainable socio-economic development of these areas (Ngala *et al*, 2015; Shuwa *et al*, 2016). The most convenient and cost-effective way to transmit power to these areas is through the use of steel poles and for optimal steel pole design that will withstand defined applied loads a numerical optimization model is inevitable (Khurmi and Gupta, 2005; Aliyu and Abejide, 2019). Traditional analysis methods for power line support structures may not adequately capture the complex stress dynamics caused by harsh environmental loads and potential malicious attacks. The vulnerability of these essential structures has highlighted the need for more robust design and assessment protocols. Seamless mild steel poles are a viable alternative to other materials due to their superior strength, durability, and lower maintenance requirements, but a thorough analysis is necessary to optimize their performance in a challenging environment like that of Borno State.

Numerical analysis deals with simulation of the design variables, searches for optimal solutions and is less expensive than experimental analysis (Biswajit, 2010; Adhikari and Bhattacharya, 2012; Umesh, 2016 ; Da Silva and Oliveira, 2018). Numerical analysis of a seamless mild steel pole for power transmission lines involves applying computational methods to evaluate its structural performance under various load conditions. This is used to ensure the pole's stability, strength, and durability for supporting low and medium-tension lines. A numerical model is defined by a mesh network, which is made up of the geometric arrangement of elements and nodes(Guoyang and Song, 2016; Gizachew and Belete, 2019). Nodes represent points at which features such as displacements and stress are calculated. The numerical packages use node numbers to serve as an identification tool in viewing solutions in structures such as deformation or deflection, stress and strain caused by applied structural and aerodynamic loads (Strivridou *et al*, 2015; Mandal *et al*, 2018; Ferroudji *et al*, 2020; Saihi and Roummani, 2020; Ferroudji, 2021; Saari *et al*, 2024).

2. Materials and Methods

American Society of Mechanical Engineers (ASME) SA-106 Grade B (British Standard B.S. 980 CDS-2) seamless mild steel pipe was selected for the pole material. The material is a low carbon steel material whose main components are carbon, silicon, manganese and small amounts of chromium, copper, nickel and molybdenum (Puwo, 2024). The selection is based on local availability, strength and cost of the material. The selected pole material has a yield strength of $8 \times 10^8 \text{ N/m}^2$, Young's Modulus E_{sp} of $2 \times 10^{11} \text{ N/m}^2$, Poisson's ratio ν of 0.33 and density ρ of 7850 kg/m^3 . The pole has two sections (Lower and Upper), with the lower section having outside diameter (OD) of 0.2032m, wall thickness (WT) of 0.008m and a length (L) of 6.7056m. The upper section has an outside diameter (od) of 0.1524m, wall thickness (wt) of 0.006m and a length (l) of 3.048m. The lower section was conically reduced to weld the upper section as shown in Figure 1.

COMSOL Multi-physics 5.2 numerical code was used to analyze the behavior of the LMTPL-SMS pole under the assumptions of Euler-Bernoulli's beam-column theory and based on geometry and material of the mild steel pole. Using the code's solid mechanics interface displacement and stress distribution response on the

pole when subjected to static, dynamic and aerodynamic loads simultaneously were computed and analyzed at an excitation frequency of 110 GHz. Electromagnetic wave code was used to solve for time harmonic electromagnetic field distribution of the pole model under the predefined loading condition.

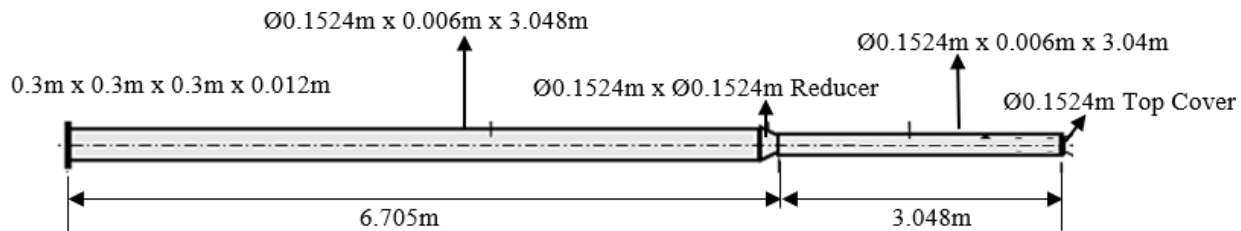


Figure 1: Geometry of the high-tension power line seamless mild steel (HTP-SMS) pole (Puwo, 2024)

The LMTPL-SMS pole geometry was created using the 3D model wizard of the numerical code. Geometrical parameters such as outside diameters (*OD* and *od*), wall thickness (*wt*) and height (*h*) were defined to build the pole in the numerical code's graphical window. The pole material property was selected and defined from the numerical code material data base as mild steel. The pole is modeled and analyzed as a beam-column under static and distributed aerodynamic loads. Boundary conditions are applied, with top of the pole considered as a free end and fixed constrained at the bottom as shown in Figure 2.

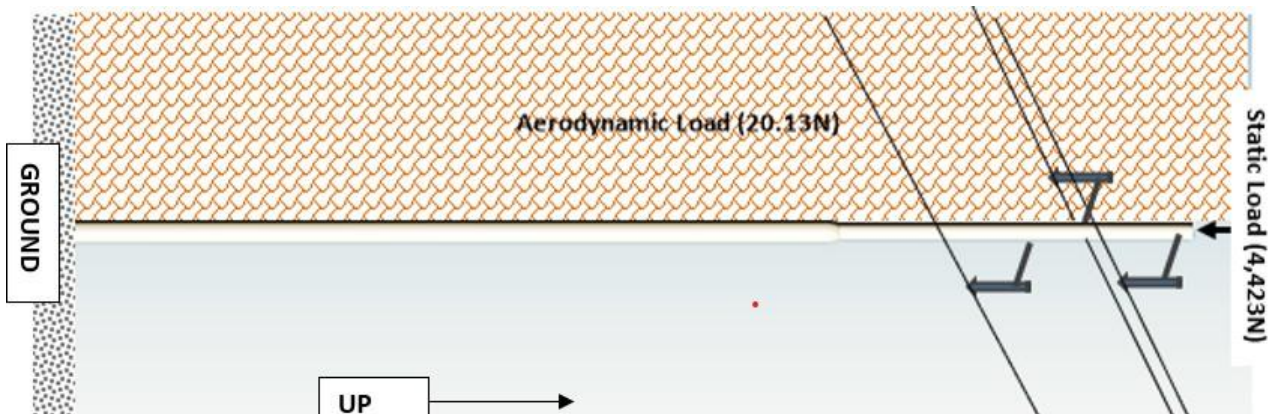


Figure 2: Loads on the HTPL-SMS pole (Abejide, 2019)

The self-weight of the LMTPL-SMS pole $W_{sp(y)}$ is determined from Equation 1 as 3,011.03N, weight of the insulators and insulators accessories $W_{ns(y)}$ determined from Equation 2 as 235.44N and weight of the conductors $W_{st(y)}$ determined from Equation 3 as 1,177.2N. The sum of these loads was the static load $W_{st(y)}$ applied at the top of the pole considered as fixed constrain along the *y* axis and determined from Equation 4 as 4,423.67N given by the summation of Equation 1, 2 and 3 (Khurmi and Gupta, 2005).

$$W_{sp(y)} = m_{sp}g \quad 1$$

$$W_{ns(y)} = m_{ns}g \quad 2$$

$$W_{cn(y)} = m_{cn}g \quad 3$$

$$W_{st(y)} = g(m_{sp} + m_{ns} + m_{cn}) \quad 4$$

Where m_{sp} is the measured mass of the LMTPL-SMS pole, m_{ns} mass of the insulator and insulator accessories, m_{cn} is the mass of the conductor the pole is expected to suspend and g is 9.81 ms^{-2} . Aerodynamic load $W_{ar(x)}$ of 20.13N due to stochastic wind is applied to the pole in the *x*, *y* and *z* planes in the user define interface of the numerical code and was determined from Equation 5 (Ferroudji et al, 2020).

$$W_{ar(x)} = A_{sp}p_wC_d \quad 5$$

Where A_{sp} is the projected area of the pole, C_d is 1.2 the drag coefficient and p_w is the wind pressure determined from Equation 6 as 34.07N. Where v_w is 23.34 ms^{-1} (52.21mph) the average stochastic wind velocity of Borno State as computed from NIME wind data from 1990-2020.

$$p_w = 0.0025(v_w)^2 \quad 6$$

Both static and aerodynamic loads are applied simultaneously on the discretized elements of the LMTPL-SMS pole to induce vibration, deformation and stresses. The pole's vibration frequency f_n , stiffness k_{sp} ,

deformation δ_{max} and stress distribution σ_{sp} are predicted based on Equations 7, 8, 9 and 10 respectively (Da Silva and Oliveira, 2018).

$$f_n = \frac{\pi}{4} \left(N_n + \frac{1}{2} \right)^2 \sqrt{\frac{g E_{sp} I_{sp}}{W_{sp} L_{y \rightarrow L}^4}} \quad 7$$

Where N_n is the mode number i.e. 1,2,3,4,.....n, W_{sp} is the weight of the LMTPTL-SMS pole determined as $3,011.03N$ ($306.935 \text{ kg} \times 9.81 \text{ ms}^{-2}$), $L_{y \rightarrow L}$ is any distance along the pole's height, and g is 9.81 ms^{-2} acceleration due to gravity.

$$k_{sp} = \frac{3 E_{sp} I_{sp}}{L_{y \rightarrow L}^3} \quad 8$$

$$\delta_{max} = \frac{[W_{st(y)} + W_{ar(x,y,z)}] L_{y \rightarrow L}^2}{3 E_{sp} I_{sp}} \quad 9$$

$$\sigma_{sp} = \frac{4(C_{efc} E_{sp} k_{rg} \pi)}{((D_1^2 - d_1^2) + (D_2^2 - d_2^2)) L_{y \rightarrow L}} \quad 10$$

Where E_{sp} is $2 \times 10^{11} \text{ N/m}^2$ Young Modulus of the LMTPTL-SMS pole material, I_{sp} is $1.0765 \times 10^{-6} \text{ m}^4$ the moment of inertia of the pole. The end fixity coefficient C_{efc} is 0.25 for a beam-column with one end fixed and the other free (Khurmi and Gupta, 2005).

The generated mesh in Figure 3 consists of 2324 domain elements, 1572 boundary elements, and 236 edge elements. Solution was computed and solved for 14,673 degrees of freedom and using the nodes as identification tool, solution to the pole's deflection, stress distribution, stiffness, natural modes of vibration in terms of corresponding frequencies due to the predefined loading conditions are obtained.

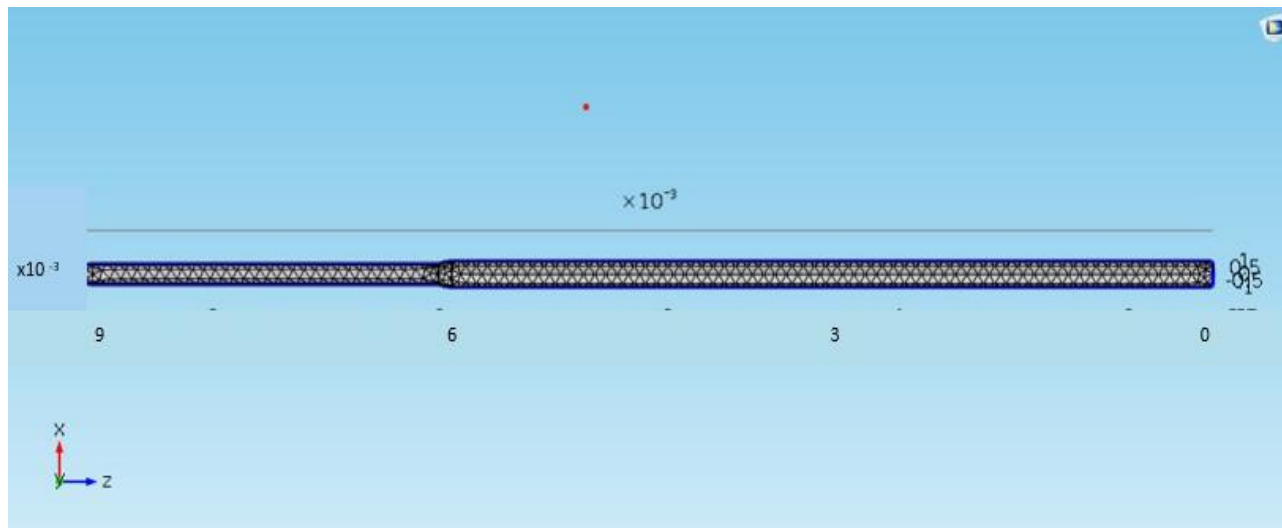


Figure 3: The generated mesh using COMSOL Multi-physics 5.2 numerical code.

The mashed LMTPTL-SMS pole geometry was solved in a frequency domain interface for time-harmonic electromagnetic field distributions. The predicted results of the LMTPTL-SMS pole deflection (displacement), stress distribution and vibration frequency response due the predefined applied loads is post processed and validated with the result form an experiment carried out on a test rig with detail is shown in Figure 4.

The experiment was performed to determine the pole's ultimate load capacity and its deformation behavior under simultaneously applied vertical and horizontal loads. A gradually increasing vertical and horizontal loads are applied at the pole's top and side using a hydraulic jack against a reaction frame. Deflectometers, pressure and strain gauges are used to measure pile head displacement, deflection, and deformation at different height of the pole (from the bottom to the top). The obtained data was plotted as a load-displacement curve to analyze the pole's performance.

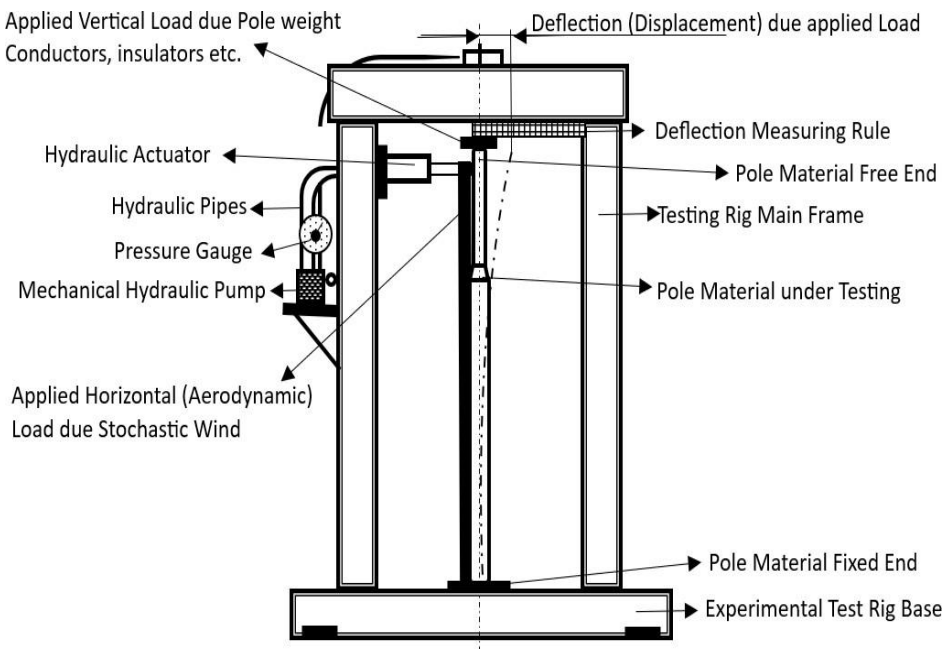


Figure 4: Details of the experimental test rig

3. Results and Discussion

Results of the numerical analysis shows the response of the LMTPTL-SMS pole as subjected to simultaneously applied static and aerodynamic loads. Figure 5 shows the meshed of the LMTPTL-SMS pole model solved in the numerical code's frequency domain interface for time harmonic electromagnetic field distributions.

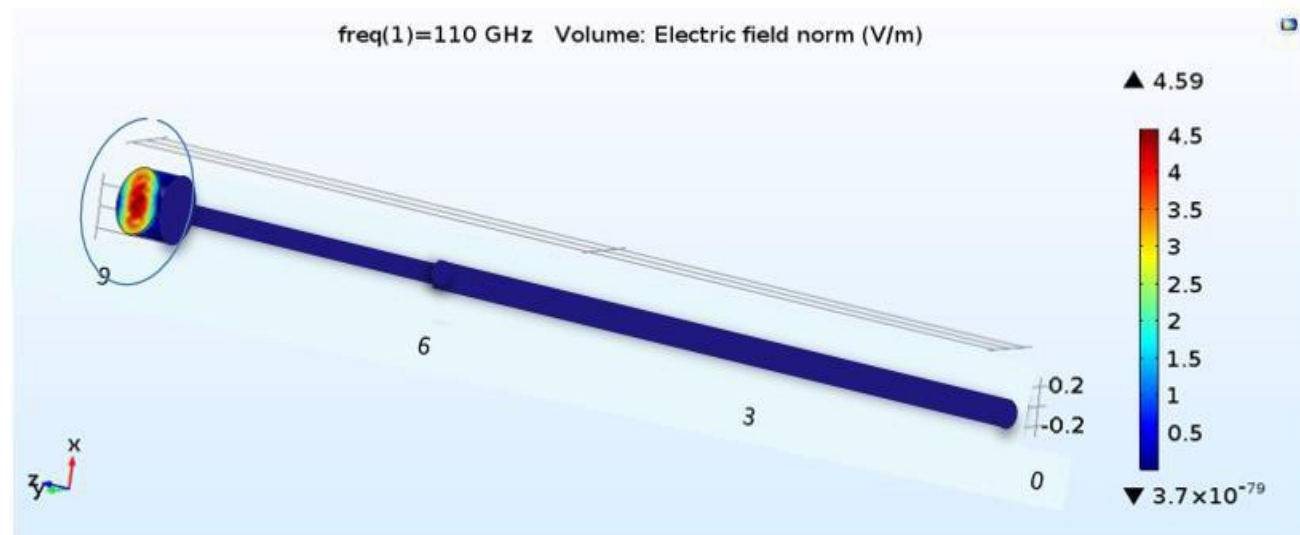


Figure 5: Frequency response of the transfer function in terms of electric field norm at 110 GHz excitation.

The result shows that minimum frequency response of the transfer function in terms of electric field norm of $3.7 \times 10^{-79} Vm^{-1}$ distributed uniformly at the circumferential boundary layer of the pole. This value increases to $4.5 \times 10^{-79} Vm^{-1}$ at the central axis of the pole through its thickness at both transfer ports. Also, there exist a similarity in the transfer function from port one to port two, which are the root and top of the pole respectively. The vibration and frequency response uniformity at the outer surface of the pole shows stability in the LMTPTL-SMS pole structure and that failure could be avoided, because under the predefined loading conditions the frequency response of the pole is less than $8.5 \times 10^{-78} Vm^{-1}$ the established response quoted of the steel pole material as quoted by the manufacturers presented by Puwo, (2024). A study by Saari et al (2024) on Estimating natural frequency of steel pipe with various geometries states showed that vibration is often the cause of structural fatigue in steel pipes and therefore piping vibration need to be closely monitored and established is at the safe range. In addition, the predicted result of the stress distribution response of the

LMTPL-SMS pole shown in Figure 6 under the predefined loads shows a maximum stress of $8.82 \times 10^7 \text{ N/m}$. This is at the pole height from 0m to 1.75m from the base of the pole in the direction of wind flow.

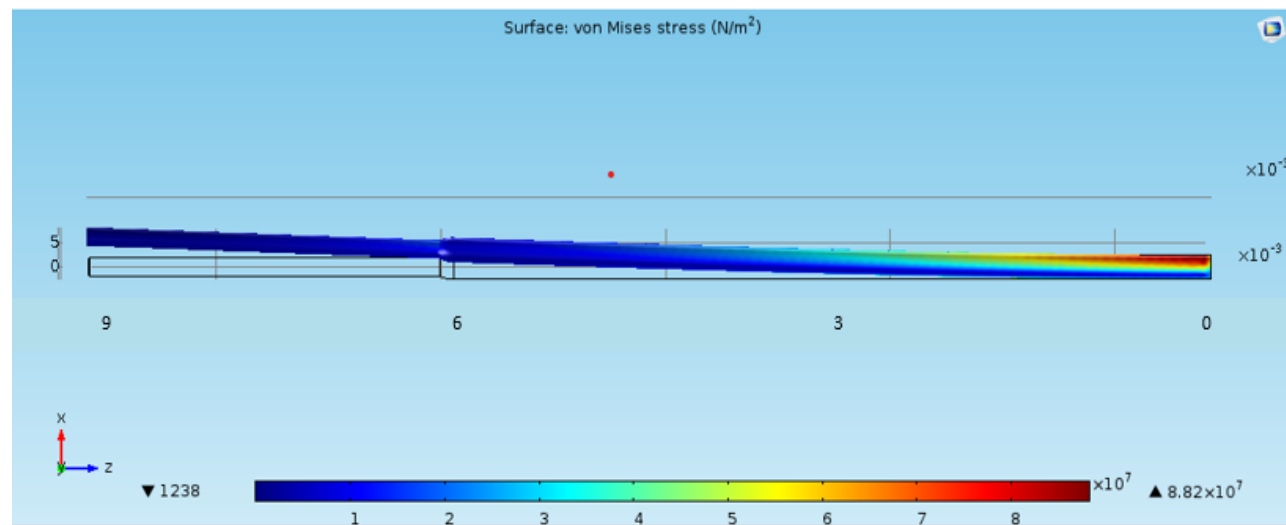


Figure 6: Predicted stress distribution of the LMTPL-SMS-pole under simultaneously applied static and aerodynamic loads.

However, the magnitude of the stress decreases along the span of the pole and decreases to $4.522 \times 10^7 \text{ N/m}$ at 3.88m and 0 N/m at 9.7536m (top of the pole). The maximum stress recorded is less than $8 \times 10^8 \text{ N/m}$ the yield strength of the pole material ((ASME) SA-106 Grade B mild steel pipe). The displacement of the LMTPL-SMS pole from its central axis along its height (from 0m at the root to 9.7536m at the top) is shown in Figure 7. The result shows gradual increases in displacement from the root (the fixed end) to the top (the free end) due to the simultaneously applied extreme loading conditions. The displacement is from 0m at the root to maximum value of 0.11m at the top. This maximum value is 22% less than 0.50m the determined critical displacement of the pole material and geometry under the predefined loading conditions. Based on the pole's material, geometry and defined boundary condition the displacement was within the elastic limit of the pole material and geometry.

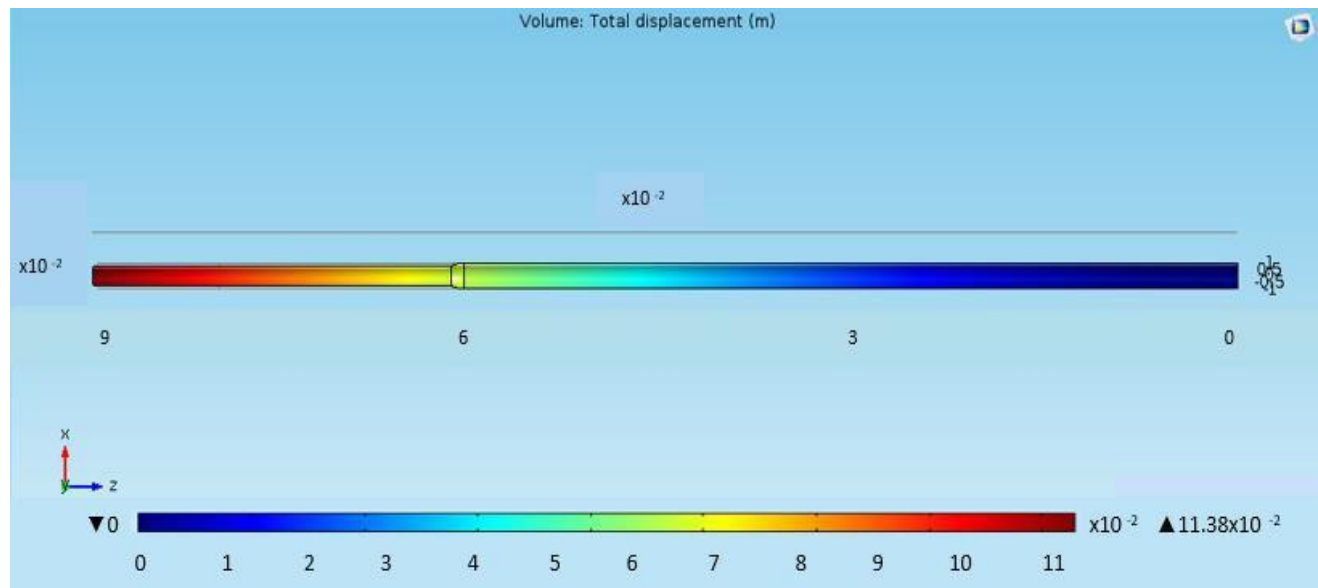


Figure 7: Predicted deformation of the LMTPL-SMS pipe due to the simultaneously applied predefine static and aerodynamic loads.

Moreover, the predicted deformation due to the extreme simultaneously applied loads was compared with a deformation from an experimental test. It was observed that the predicted values were in agreement with the values obtained from the experimental test carried out in Figure 8 with a *P* value of 0.989 obtained from the statical *F* Test carried out in Microsoft Excel. The *P* value is greater than 0.5 thus there is no significant difference between the predicted deformation and the experimental test carried out by Ashaf et al 2005.

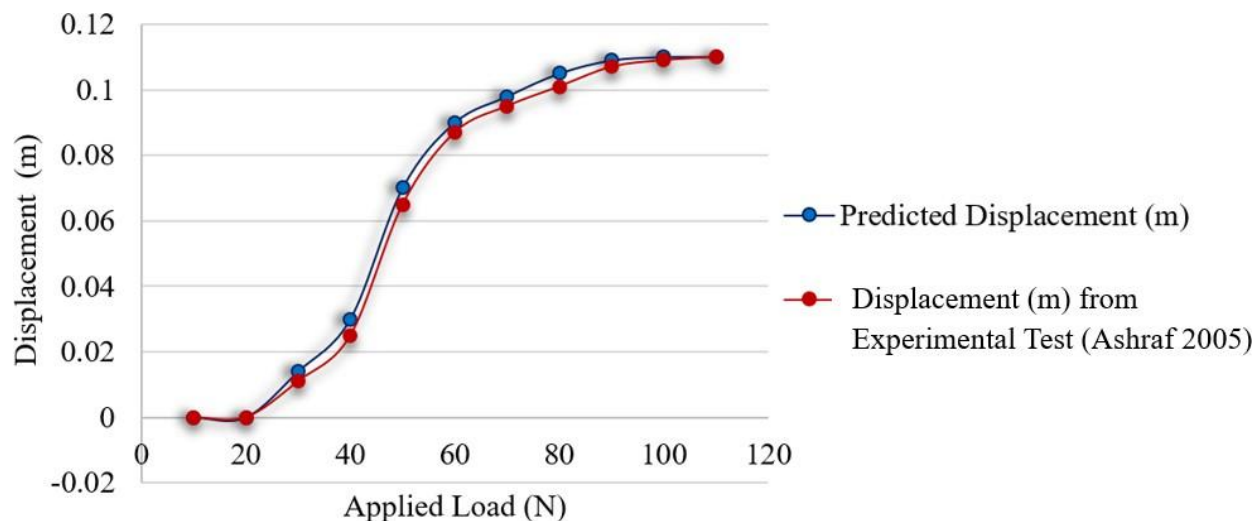


Figure 8: Validation of displacement along the LMTPL-SMS pole span due the applied loading conditions

4. Conclusion

Numerical analysis of the low and medium tension power transmission line seamless mild steel (LMTPL-SMS) pole was successfully carried out using the numerical code COMSOL Multi-physics 5.2. The pole's response to simultaneously applied predefined loading conditions was examined and the results in terms of vibration, stress and displacement were analyzed. The predicted response of the pole material with regards to vibration, stress and displacement were found to be within the safe limits of the selected pole material (ASME SA-106 Grade B mild steel) considering the pole's mechanical properties and geometry. The statistical tool F-Test used to validate the predicted results with an experimental one shows no significant difference between the two results. Thus, the selected pole material was reliable and is suitable for low and medium tension power transmission network in Borno State, Nigeria.

References

Aliyu, M. and Abejide, OS. 2019. Finite Element Modelling of Steel Poles for Power Production and Transmissions. Nigerian Journal of Technology (NIJOTECH), 38(4):840-847.

Abejide, A. 2019. Finite Element Modelling of Steel Poles for Power Production and Transmissions. Nigerian Journal of Technology (NIJOTECH), 38(4):840-847.

Adhikari, S. and Bhattacharya, S. 2012. Dynamic Analysis of Wind Turbine Towers on Flexible Foundations. Journal of Shocks and Vibrations, 19:37-56.

Ashraf, M., Ahmad, H. M. and Saddiqi, Z. A. 2005. A Study of Power Transmission Poles, Asian Journal of Civil Engineering (Building and Housing), 6(6):511-532

Biswajit, B. 2010. Tower Design and Analysis. WIT Transaction on State of the Art in Science and Engineering, 44:527-558.

Da Silva, B.G.S. and Oliveira, B.A.S. 2018. "Evaluation of the Nondeterministic Dynamic Structural Response of Three-Timensional wind Turbine Steel Towers. Journal of Wind Energy, 40:364-377.

David, J. 2005. Engineering Material Standard Code Book. New York: M. Harison Inc.

Ferroudji, F. 2021. Numerical Model Analysis of a 850 KW Turbine Steel Tower. International Review of Applied Science and Engineering, 12(1):10-18.

Ferroudji, F., Lakhdar, S. and Khayra, R. 2020. Numerical Simulations on Static and Dynamic Response of Full-scale Mast Structures for Hdarrieus Wind Turbine. SAGE Wind Engineering, 45(4):822-837.

Gizachew, DT. and Belete, S. 2019. Upwind 2MW Horizontal Axis Wind Turbine Tower Design and Analysis. Science Publishing Group, 7(5):111-131.

Guoyang, X. and Song, X. 2016. Simulation Analysis of Universal Fatigue Life of Tower Load of Horizontal Axial Force Wind Turbine. Journal of Gansu Science, 28(4):115-118.

Khurmi, RS. and Gupta, JK. 2005. Machine Design. New Delhi: Eurasia Publishing House (PVT) Ltd.

Mandal, AK., Rana, KB. and Tripathi, . 2018. Experimental and Numerical Analysis on Small Wind Turbines: A Review. International Journal of Applied Engineering Research, 13(8):97-111.

Ngala, GM., Shuwa, M., Oumarou, MB. and Muhammad, AB.. 2015. A CFD Analysis of a Micro Horizontal Axis Wind Turbine Blade Aerodynamics. Arid Zone Journal of Engineering, Technology and Environment, 11:13-23.

Nweke, FU., Anyigor, IS., Iburu, U. and Ekpe, J. 2017. Overhead Lines for Transmission and Distribution of Power System and its Consequences in Nigeria. International Digital Organization for Scientific Research (IDOSR), 2(3):1-7.

Oyejide, SA., Adejumobi, IA., Wara, ST. and Ajisegiri, ESA. 2014. Development of a Grid-Based Rural Electrification Design: A Case Study of Ishashi and Ilogbo Communities in Lagos State. Journal of Electrical and Electronic Engineering (IOSR-JEEE), 9:12-21.

Puwo, H. 2024. Material Parameter Handbook. Guancheng: Henan Puwo Metal Materials Company Limited.

Saari, NF., Putra, A., Irianto, RMD., Muhammad AZ., Roszaidi R., Nawal AA. and Safarudin H. 2024. Estimating natural frequency of pipe with various geometries: Improvement of frequency factors. Heliyon Research article, Elsevier Ltd, 10(4):1-17.

Saihi, L and Roummani, K. 2020. Numerical simulations on static and dynamic response of full-scale mast structures for Hdarrieus wind turbine. SAGE Journal of Wind Engineering, 45(4):822-837.

Shuwa, M., Ngala, GM. and Maina, M. 2016. Development and Performance Test of a Micro Horizontal Axis Wind Turbine Blade. International Journal of Engineering Research and Application, 6(2):11-17.

Strivridou, N., Eottasakis, E. and Saniotopoulos, C. 2015. Finite Element Analysis and Comparative Study of Welded connection of Wind Turbine Towers Under Fatigue Loading. International Journal of Applied Sciences , 8:489-500.

Umesh, KN. 2016. Design and Analysis of 2-MW Wind Turbine Tower. International Journal of Mechanical and Production Engineering, 4(10):13-17.

Wagner, HJ. and Mathur, J. 2018. Introduction to Wind Energy Systems. Berlin: Springer.

WAPA. 2021. Standard 5 Transmission Lines Steel Pole Structures. New York: Western Area Power Administration (WAPA).